Density expansion of transport coefficients on a 2D site-disordered lattice. II

1987 J. Phys. A: Math. Gen. 20 5335

(http://iopscience.iop.org/0305-4470/20/15/045)

J. Phys. A: Math. Gen. **20** (1987) 5335–5350. Printed in the UK

Density expansion of transport coefficients on a 2D site-disordered lattice: II

M H Ernst†, Th M Nieuwenhuizen‡ and P F J van Velthoven§

† Institute for Physical Science and Technology, University of Maryland, College Park, MD 20742, USA

‡ Institut für Theoretische Physik A, RWTH, Templergraben 55, 5100 Aachen, Federal Republic of Germany

§ Instituut voor Theoretische Fysica, State University, PO Box 80.006, 3508 TA Utrecht, The Netherlands

Received 8 December 1986, in final form 7 May 1987

Abstract. For a hopping model on a square lattice with a fraction c of sites randomly replaced by impurities, the static conductivity and diffusion coefficients can be expanded in powers of the concentration c. Here we calculate the exact coefficients of $O(c)$ and $O(c^2)$ using analytical and numerical methods, and the results are compared with computer simulations.

1. Introduction

In a previous paper (Nieuwenhuizen *et al* 1987, hereafter referred to as I), we have developed a systematic kinetic theory approach for calculating transport properties in diffusive systems with static disorder, partly based on the method of Lifshitz (1964). The theory was applied to a random walk (RW) with nearest-neighbour (NN) hops on a square lattice, with a fraction c of sites, chosen at random, replaced by impurities. The impurity at site n determines the jump rate σ into the site n. Depending on their properties impurities may decrease ($\sigma < 1$) or increase ($\sigma > 1$) the average transport properties. For $\sigma = 0$ the impurity sites are blocked and one has the standard site percolation model.

The model is very different from the random jump rate model, where the impurity at site n determines the jump rate out of the size n. For the latter model the diffusion coefficient $D(c)$ is known exactly for arbitrary dimensionality (Haus and Kehr 1987). The percolation transition, however, always occurs at $c = 1$, as in the one-dimensional case.

For our RW model with site disorder, expressions were derived for the response function and the transport coefficients, exact to $O(c^2)$ in the impurity concentration. In this paper the expressions will be evaluated, partly analytically, partly numerically, to obtain the diffusion coefficient and conductivity for the RW model on the site-disordered lattice described above.

We briefly describe the model and recall the necessary results and definitions of I. The system under consideration is a square lattice with unit lattice distance, N sites and with periodic boundary conditions. To every site $n = \{n_x, n_y\}$ a random variable $\psi_n = 1 - bc_n$ is assigned, where $\psi_n = 1 - b \equiv \sigma$ (where $\sigma \geqslant 0$) with probability c for an

0305-4470/87/155335+16$02.50

impurity site ($c_n = 1$) and where $\psi_n = 1$ with probability $(1-c)$ for a host lattice site ($c_n = 0$). If $\sigma = 0$ (or $b = 1$) the impurity sites are inaccessible or excluded to the RW, corresponding to the standard site percolation model. We use the formulation of a continuous time dynamics, where the probability distribution $p_n(t)$ for the RW is described by the master equation

$$\dot{p}_n = \tfrac{1}{4}\sum_{\rho}(\psi_n p_{n+\rho} - \psi_{n+\rho} p_n). \tag{1.1}$$

The relation of this model to the ordinary discrete-time random walk was given in I. The site percolation model ($\sigma = 0$) can also be considered as a lattice Lorentz gas (Keyes and Lyklema 1982, Nieuwenhuizen *et al* 1986, Frenkel 1986).

The transport properties of interest in this paper are the diffusion coefficient $D(c)$, defined through the long-time behaviour of the mean square displacement $\langle n_x^2\rangle \simeq 2D(c)t$ $(t \to \infty)$, and the static conductivity $\Sigma(c) = \langle\psi\rangle D(c)$, where $\langle\psi\rangle = 1 - bc$ is the effective free-volume fraction or 'porosity' of the system.

In I we obtained an expression for the frequency-dependent conductivity $\Xi(z, c)$ and for the Laplace transform of the velocity autocorrelation function (VACF) $\Phi(z, c)$, exact to $O(c^2)$ in the concentration of impurities. Their limit as $z \to 0$ reduces to the static conductivity $\Sigma(c) = \Xi(0, c)$ and diffusion coefficient $D(c) = \Phi(0, c)$. The expressions are

$$\Xi(z, c) = \langle\psi\rangle\Phi(z, c) = \tfrac{1}{4} - ct_3(z) + c^2[K_{33}(z) + Q_3(z)] + O(c^3). \tag{1.2}$$

Here t_3, K_{33} and Q_3 are elements of 5×5 matrices and of a 5-vector $\boldsymbol{Q}$, labelled $i, j = [0, 1, 2, 3, 4]$, defined as

$$\begin{aligned} \boldsymbol{K}(z) &= \sum_{n\neq 0}\boldsymbol{k}(n, z) = \sum_{n\neq 0}[\boldsymbol{t}^{-1}(z) + \boldsymbol{g}(n, z)]^{-1}\boldsymbol{g}(n, z)\boldsymbol{t}(z) \\ \boldsymbol{Q}(z) &= [\boldsymbol{t}^{-1}(z) + \boldsymbol{g}(\rho_1, z)]^{-1}\boldsymbol{a}(\rho_1)b \end{aligned} \tag{1.3}$$

where $\rho_1 = \{1, 0\}$ is a NN site of the origin, and the column 5-vector $\boldsymbol{a}(\rho_1)$ has the elements $\{0, -\frac{1}{4}, \frac{1}{4}, \frac{1}{2}, 0\}$. The lattice Green function $\boldsymbol{g}(n, z)$ is a real 5×5 matrix, the elements of which are linear combinations (with m equal to n or one of its NN or NNN sites) of standard lattice Green functions $G_m(z)$, denoting the probability for a displacement m on a uniform lattice. They have the explicit form

$$\boldsymbol{g}(n, z) = \boldsymbol{S}\int_q [z + \omega(q)]^{-1}\exp(-\mathrm{i}qn)\tilde{\boldsymbol{e}}(q)\boldsymbol{e}(q)\boldsymbol{S}$$

where the integration sign denotes an average over the first Brillouin zone of the square lattice with q_x, $q_y \in [-\pi, \pi]$ and weight $(4\pi^2)^{-1}$. The basis vectors are defined as

$$\begin{aligned} \boldsymbol{e}(q) &= \{1, e_1, e_2, e_3, e_4\} \\ \tilde{\boldsymbol{e}}(q) &= \{0, e_1 - 1, e_2, e_3, e_4\} \end{aligned} \tag{1.4a}$$

with

$$\begin{aligned} e_1(q) &= \omega(q) = 1 - \tfrac{1}{2}\cos q_x - \tfrac{1}{2}\cos q_y \\ e_2(q) &= \tfrac{1}{2}\cos q_x - \tfrac{1}{2}\cos q_y \qquad e_3(q) = \sin q_x \qquad e_4(q) = \sin q_y. \end{aligned} \tag{1.4b}$$

The transformation matrix $\boldsymbol{S}$ is diagonal with elements $\{1, 1, 1, \mathrm{i}, \mathrm{i}\}$ with $\mathrm{i} = \sqrt{-1}$. This matrix $\boldsymbol{S}$ makes all matrix elements of $\boldsymbol{g}(n, z)$ real. The matrix elements of the diagonal matrix $\boldsymbol{t}(z)$ account for the sum of all possible RW on a uniform lattice that return to

their point of origin. In kinetic theory language these contributions are called 'repeated ring collisions'. Their explicit form is

$$\boldsymbol{t}(z) = \mathrm{diag}\{1, t_1, t_2, t_3, t_4\} \tag{1.5a}$$

with

$$(t_j(z))^{-1} = \begin{cases} 1/b - g_{ij}(0, z) & (j = 1, 2) \\ 2/b + g_{33}(0, z) & (j = 3, 4). \end{cases} \tag{1.5b}$$

To obtain explicit values for diffusion coefficient and conductivity one has to calculate lattice Green functions for all sites, invert the matrices $[\boldsymbol{t}^{-1} + \boldsymbol{g}(n)]$ and carry out the lattice summation in (1.2). In §§ 2 and 3 we compute the $O(c)$ and $O(c^2)$ contributions respectively to the diffusion coefficient. Section 4 contains a discussion of the results and a comparison with computer simulations. Analytic results for the Green functions are developed in appendix 1 and for a special lattice sum in appendix 2.

2. Transport coefficients to O(*c*)

In this section we concentrate on the contribution linear in the impurity concentration c that was obtained by summing the so-called 'repeated ring collisions' of the RW with a single impurity.

The expression to be analysed follows from (1.2) and (1.5) as

$$\Xi(z) = \tfrac{1}{4} - \tfrac{1}{2}\, cb/[1 - bI(z)] \tag{2.1}$$

where $I(z)$ is the ring collision integral

$$I(z) \equiv -\tfrac{1}{2} g_{33}(0, z) = \tfrac{1}{2} \int_q (\sin q_x)^2/[z + \omega(q)]. \tag{2.2}$$

For the square lattice and in the static limit ($z \to 0$) this integral can be calculated by introducing new integration variables $\alpha = \frac{1}{2}(q_x + q_y)$ and $\beta = \frac{1}{2}(q_x - q_y)$ and by using the symmetry of the integrand to reduce the resulting integration region to one quarter. The result is

$$\begin{aligned} I(0) &= (1/\pi^2) \int_0^\pi \int_0^\pi \mathrm{d}\alpha\, \mathrm{d}\beta\, \cos^2 \alpha (1 - \cos^2 \beta)/(1 - \cos \alpha \cos \beta) \\ &= 1 - 2/\pi. \end{aligned} \tag{2.3}$$

The DC conductivity and diffusion coefficient are then given by

$$\Sigma(c) = (1 - bc) D(c) = \tfrac{1}{4} - \tfrac{1}{2} cb/(1 - bI(0)) + O(c^2). \tag{2.4}$$

Here $D(0) = \frac{1}{4}$ is the diffusion coefficient of the impurity free lattice with $I(0) = 1 - 2/\pi$.

For the percolation case (blocked sites, non-conducting impurities) the parameter $b = 1$ and the jump rate into the impurity site is $\sigma = 1 - b = 0$. Then the static conductivity simplifies to $\Sigma(c) = (1 - \pi c)/4$ as already derived by Izyumov (1966) and Harris and Kirkpatrick (1977) in the context of random ferromagnets.

3. Transport coefficients to $O(c^2)$

3.1. Reduction to 3×3 matrices

The $O(c^2)$ contribution involves the more difficult problem of the interactions of a RW with two impurities, and requires the evaluation of the lattice sum (1.2) in the limit $z \to 0$. The static transport coefficients have the following expansion in powers of the impurity concentration c:

$$\begin{aligned} \Sigma(c) &= \tfrac{1}{4}(1+\beta_1 c+\beta_2 c^2+\ldots) \\ D(c) &= \tfrac{1}{4}(1+\alpha_1 c+\alpha_2 c^2+\ldots). \end{aligned} \tag{3.1}$$

Since $\langle\psi\rangle = 1-bc$ the expansion coefficients are related as $\beta_1 = \alpha_1 - b$ and $\beta_2 = \alpha_2 - b\alpha_1$ with

$$\begin{aligned} \beta_1 &= -4t_3(0) = -2b/[1-b(1-2/\pi)] \\ \beta_2 &= 4[K_{33}(0)+Q_3(0)]. \end{aligned} \tag{3.2}$$

The results for the $O(c)$ coefficients α_1 and β_1 have already been given through (2.4). This section is devoted to the calculation of α_2 and β_2. We start with the lattice sum in (1.3). The reflection symmetries described in appendix 2 of I guarantee that $k_{33}(\{n_x, n_y\}, z)$ only depends on the absolute values $|n_x|$ and $|n_y|$, and equals $k_{44}(\{n_y, n_x\}, z)$. Symmetrisation in n_x and n_y of the summand in (1.3) yields

$$K_{33}(z) = \sum_{n\neq 0} k_{33}(n, z) = \tfrac{1}{2}\sum_{n\neq 0}[k_{33}(n, z)+k_{44}(n, z)] \tag{3.3}$$

and the square symmetry allows us to restrict the summation to one eighth of the $\{n_x, n_y\}$ plane ($n_x \geqslant n_y \geqslant 0$).

In order to study the 5×5 matrix $\boldsymbol{K}(z)$ and the 5-vector $\boldsymbol{Q}(z)$ in (1.3) we need to introduce some notation:

$$\begin{aligned} \boldsymbol{r}(n, z) &= \boldsymbol{g}(n, z)\boldsymbol{t}(z) \\ \boldsymbol{\Gamma}(n, z) &= [\boldsymbol{t}^{-1}(z)+\boldsymbol{g}(n, z)]^{-1} = \boldsymbol{t}(z)[\mathbf{1}+\boldsymbol{r}(n, z)]^{-1}. \end{aligned} \tag{3.4}$$

Hence

$$\begin{aligned} \boldsymbol{k}(n, z) &\equiv \boldsymbol{\Gamma}(n, z)\boldsymbol{r}(n, z) = \boldsymbol{t}(z)-\boldsymbol{\Gamma}(n, z) \\ &= \boldsymbol{t}(z)\boldsymbol{r}(n, z)-\boldsymbol{h}(n, z) \end{aligned} \tag{3.5}$$

with

$$\begin{aligned} \boldsymbol{h}(n, z) &\equiv \boldsymbol{\Gamma}(n, z)\boldsymbol{r}^2(n, z) \\ &= \boldsymbol{\Gamma}(n, z)-\boldsymbol{t}(z)+\boldsymbol{t}(z)\boldsymbol{r}(n, z). \end{aligned} \tag{3.6}$$

The 5-vector $\boldsymbol{Q}(z)$ in (1.3) can be written as

$$Q_j(z) = (\boldsymbol{\Gamma}(\rho_1, z)\boldsymbol{r}(\rho_1, 0))_{j1}. \tag{3.7}$$

Here we have made use of (A1.7) and the equality $t_1(0) = b$ (see (A1.10)), which implies

$$a_j(\rho_1)b = g_{j1}(\rho_1, 0)b = r_{j1}(\rho_1, 0). \tag{3.8}$$

Consider first the inversion of the 5×5 matrix $\boldsymbol{\Gamma}^{-1}(n, z)$ with labels $i, j \in \{0, 1, 2, 3, 4\}$, where $\boldsymbol{t}(z)$ is a diagonal matrix, defined in (1.5), and $\boldsymbol{g}(n, z)$ is defined in (1.4). The

$(0j)$ elements of $\boldsymbol{g}(n, z)$ are vanishing on account of (1.4*a*). Hence $g_{0j}(n, z) = r_{0j}(n, z) = 0$, which implies that $\Gamma_{0j}(n, z) = 0$ for $j \in \{1, 2, 3, 4\}$. Next we note that $\boldsymbol{\Gamma}(n, z)$ in (3.6) is multiplied on the right by $\boldsymbol{r}(n, z)$, the zeroth row of which is vanishing also. Consequently, the zeroth column $\Gamma_{j0}(n, z)$ never contributes to any of the matrix elements of $\boldsymbol{k}(n, z)$ in (3.5). We can always restrict ourselves to the (1234) subspace and only work with 4×4 matrices with labels $i, j \in \{1, 2, 3, 4\}$.

A further reduction to 3×3 matrices can be achieved by setting $z = 0$ in (3.4). Consider the first column of $\boldsymbol{\Gamma}^{-1}(n, z)$. Then it follows from (1.5), (A1.10), (3.4) and (A1.7) that

$$\begin{aligned}(\boldsymbol{\Gamma}^{-1}(n, 0))_{j1} &= \delta_{j1} t_1^{-1}(0) + g_{j1}(n, 0) \\ &= \delta_{j1} b^{-1} + a_j(\rho)\delta_{n\rho}. \end{aligned} \tag{3.9}$$

In this expression ρ stands for one of the NN lattice vectors ρ_i with $i = 1, 2, 3, 4$. Thus if $n \neq \rho$, we have $\Gamma_{j1}(n, 0) = b\delta_{j1}$ and the matrix elements $\Gamma_{ij}(n, 0)$ with $i, j \in \{2, 3, 4\}$ and $n \neq \rho$ do not depend on the quantities in (3.7). Consequently, $\Gamma_{ij}(n, 0)$ and $(\boldsymbol{\Gamma}(n, 0)\boldsymbol{r}(n, 0))_{ij}$ for $n \neq \rho$ with $i, j \in \{2, 3, 4\}$ can be calculated from the 3×3 matrices $\boldsymbol{g}(n, 0)$ and $\boldsymbol{r}(n, 0)$, restricted to the (234) subspace; for sites $n \neq 0$ and $n \neq \rho$ we can always work with 3×3 matrices with labels $i, j \in \{2, 3, 4\}$.

3.2. Evaluation of matrix elements

In the remaining part of § 3 we drop the argument, $z = 0$, e.g. $\boldsymbol{\Gamma}(n) = \boldsymbol{\Gamma}(n, 0)$, $\boldsymbol{t} = \boldsymbol{t}(0)$, etc.

We first consider contributions from nearest-neighbour sites ($n = \rho$), which require a separate discussion, because $\boldsymbol{\Gamma}(\rho)$ cannot be reduced to the (234) subspace. Nearest-neighbour terms appear in Q_3 of (3.7) and in $k_{33}(\rho)$ and $k_{44}(\rho)$ of (3.4). On account of (3.5) the Q term reduces to

$$Q_3 = Q_3(0) = -\Gamma_{31}(\rho_1). \tag{3.10}$$

In the further discussion of $\boldsymbol{\Gamma}(\rho)$ and $\boldsymbol{r}(\rho) = \boldsymbol{g}(\rho)\boldsymbol{t}$ from NN sites we can restrict our considerations to the site $\rho_1 = \{1, 0\}$ because of square symmetry. The inverse matrix $\boldsymbol{\Gamma}^{-1}(\rho_1) = \boldsymbol{t}^{-1} + \boldsymbol{g}(\rho_1)$ is given through (1.5) and (A1.10) and is

$$\boldsymbol{\Gamma}^{-1}(\rho_1) = \begin{bmatrix} 1/b - \frac{1}{4} & \frac{5}{4} - 4/\pi & 4/\pi - \frac{3}{2} & 0 \\ \frac{1}{4} & 1/b - \frac{1}{4} & \frac{5}{2} - 8/\pi & 0 \\ \frac{1}{2} & \frac{5}{2} - 8/\pi & 2/b - 16/\pi - 6 & 0 \\ 0 & 0 & 0 & 2/b - 1 \end{bmatrix}. \tag{3.11}$$

Evaluation of $\Gamma(\rho_1)$ requires at most inversion of a 3×3 matrix-involving determinant and minors of (3.11). We only list the explicit results as far as they are needed in subsequent calculations:

$$\begin{aligned} \Gamma_{31}(\rho_1) &= [-(2b)^{-1} + \tfrac{3}{4} - 2/\pi]/\mu(\rho_1) \\ \Gamma_{33}(\rho_1) &= [b^{-2} - (2b)^{-1} - \tfrac{1}{4} + 1/\pi]/\mu(\rho_1) \\ \Gamma_{44}(\rho_1) &= b/(2-b) \end{aligned} \tag{3.12}$$

where $\mu(\rho_1)$ is the determinant of the 3×3 matrix in the upper left corner of (3.11).

Next we consider $\boldsymbol{\Gamma}(n, 0)$ for more distant sites, where we can restrict ourselves to the (234) subspace. The evaluation requires the lattice Green functions $\boldsymbol{g}(n, 0)$. For the neighbour sites $\{n_x, n_y\}$ with $|n_x| + |n_y| \leq 4$ we have listed the values of the matrix

elements in table 3. Combination of these expressions with $\boldsymbol{t}(0)$ in (1.5) yields the 3×3 matrix $\boldsymbol{\Gamma}^{-1}(n,0)$. For more distant sites the analytic calculation of $\boldsymbol{g}(n,0)$ readily becomes too cumbersome and the integrals $g_{ij}(n,0)$ are evaluated numerically, as described in appendix A1.2. The required matrix inversions and multiplications for all sites n are performed numerically.

3.3. Analysis of the lattice sums

In evaluating the lattice sum $\boldsymbol{K}(0)$ in (3.4) it is not permitted to interchange the limit $z\to 0$ with the lattice summation. The reason is that the most dominant matrix elements of $\boldsymbol{r}(n,0)$ behave as $|\Gamma_{ij}(n,0)|\sim O(|n|^{-2})$ for $|n|\gg 1$ with $|n|^2=n_x^2+n_y^2$, as discussed in (A1.16). Consequently the 2D lattice sum $\Sigma\,|\boldsymbol{k}(n,0)|$ diverges logarithmically. Furthermore $\Sigma\,|\boldsymbol{k}(n,z)|$ cannot be evaluated analytically and in its present form is not suitable for numerical evaluation. However, we can increase the rate of convergence of the lattice sum by subtracting the slowly converging part, which can be evaluated analytically. This can be done by inserting the third equality of (3.5) into the lattice sum:

$$\begin{aligned}\boldsymbol{K}(z)&=\sum_{n\neq 0}[\boldsymbol{t}(z)\boldsymbol{r}(n,z)-\boldsymbol{h}(n,z)]\\&=-\boldsymbol{t}(z)\boldsymbol{r}(0,z)-\sum_{n\neq 0}\boldsymbol{\Gamma}(n,z)\boldsymbol{r}^2(n,z).\end{aligned}\tag{3.13}$$

The n summation of the second term can be performed numerically because the summand decreases as $|n|^{-4}$ for large $|n|$. The summation of the first term was performed analytically using the relations

$$\begin{aligned}\sum_{n\neq 0}\boldsymbol{r}(n,z)&=\boldsymbol{S}_c\sum_{n\neq 0}\int[z+\omega(q)]^{-1}\exp(-\mathrm{i}qn)\tilde{\boldsymbol{e}}(q)\boldsymbol{e}(q)\boldsymbol{S}_c\boldsymbol{t}(z)\\&=-\boldsymbol{r}(0,z).\end{aligned}\tag{3.14}$$

In the last equality we carried out the lattice summation with the help of $\Sigma_{n\neq 0}\exp(-\mathrm{i}qn)=N\delta_{q0}-1\ldots$ and used relations (3.4) and (1.4). Then the limit $z\to 0$ can be taken under the summation sign and we find for the relevant (33) element:

$$K_{33}(0)=-t_3r_{33}(0)-\sum_{n\neq 0}(\boldsymbol{\Gamma}(n)\boldsymbol{r}^2(n))_{33}.\tag{3.15}$$

The large-n behaviour of the summand in (3.15) can be obtained from the relation $\boldsymbol{\Gamma}(n)\simeq\boldsymbol{t}$ as $|n|\gg 1$ and (A1.16) and reduces to

$$(\boldsymbol{t}\boldsymbol{r}^2(n))_{33}\simeq(4/\pi^2)t_3^3|n|^{-4}\qquad(|n|\gg 1).$$

Therefore the 2D lattice sum in (3.15) converges only slowly. The rate of convergence can be increased considerably by performing the sum $\Sigma\,\boldsymbol{r}^2(n)$ analytically, as has been done in equation (A2.5). If $\boldsymbol{\Gamma}(n)$ in (3.15) is written as $\boldsymbol{\Gamma}(n)=\boldsymbol{t}-\boldsymbol{\Gamma}(n)\boldsymbol{r}(n)$ (see (3.5)), then (3.4) and (A1.9) give $r_{33}(0)=(4/\pi-2)t_3$ and the lattice sum becomes

$$K_{33}(0)=t_3^2(2-4/\pi)+t_3^2\sum_{j=1}^{3}t_j\nu_j+\sum_{n\neq 0}(\boldsymbol{\Gamma}(n)\boldsymbol{r}^3(n))_{33}\tag{3.16}$$

with coefficients ν_j following from (A2.5):

$$\begin{aligned}\nu_1&=\tfrac{3}{2}-4/\pi\\\nu_2&=\tfrac{15}{2}-24/\pi\\\nu_3&=16/\pi^2+48/\pi-18.\end{aligned}\tag{3.17}$$

Next we consider the large-$|n|$ behaviour of the summand, which follows from (A1.16)

and (3.4) as

$$(\Gamma(n)\boldsymbol{r}^3(n))_{33} \simeq (8/\pi^3)t_3^4(n_x^2 - n_y^2)|n|^{-8} + O(|n|^{-7}).$$

Since this expression changes sign upon interchanging n_x and n_y, its leading $O(|n|^{-6})$ contribution to the lattice sum (3.16) vanishes, and the summand decreases at least as fast as $|n|^{-7}$ for $|n| \gg 1$. Thus, the lattice sum in (3.16) is rapidly converging and will be used for numerical calculations.

Let $K_{33}^{(N)}(0)$ denote the value of $K_{33}(0)$ in (3.16), obtained by performing the lattice sum over the diamond-shaped region $|n_x|+|n_y| \leq N$, containing approximately $N^2/2$ sites. Then one can use the formula

$$K_{33}(0) = K_{33}^{(N)}(0) + r_0 N^{-5} \tag{3.18}$$

as an extrapolation formula for large N. The constant r_0 appearing in the remainder can be estimated by considering $K_{33}^{(N)}(0)$ for different values of N, where for small N the estimate for r_0 will depend on N. We have used this method in our calculation, and illustrated it in table 1 for the percolation case ($b = 1$). The more accurate calculations, reported in I for the percolation case, allow us to estimate the relative error in this procedure to be $1:10^{-4}$. In table 2 we have summarised the values of

Table 1. Lattice sum in (3.17) for $|n_x|+|n_y| \leq N$ and its extrapolation on (3.18) for $b = 1$.

N	$K_{33}^{(N)}(0)$	$K_{33}^{\text{extr}}(0)$
1	−0.000 37	−0.000 37
2	−0.220 03	−0.227 11
3	−0.224 14	−0.224 76
4	−0.224 66	−0.224 83

Table 2. $O(c^2)$ coefficients for different impurity jump rates $\sigma = 1 - b$.

b	$K_{33}(0)$	$Q_3(0)$	β_2	α_2
1.000	−0.2248	0.5463	1.2858	−0.8558
0.900	−0.0532	0.4087	1.4223	−0.1750
0.800	0.0202	0.2980	1.2730	0.1084
0.700	0.0453	0.2105	1.0231	0.1988
0.600	0.0470	0.1427	0.7591	0.1983
0.500	0.0387	0.0915	0.5207	0.1597
0.400	0.0271	0.0541	0.3248	0.1104
0.300	0.0160	0.0282	0.1766	0.0645
0.200	0.0073	0.0116	0.0754	0.0292
0.100	0.0018	0.0027	0.0181	0.0073
−0.111 11	0.0022	0.0028	0.0202	0.0089
−0.250	0.0109	0.0131	0.0960	0.0439
−0.428 57	0.0307	0.0341	0.2593	0.1251
−0.666 67	0.0695	0.0709	0.5617	0.2906
−1.000	0.1415	0.1306	1.0888	0.6218
−1.500	0.2731	0.2240	1.9884	0.1326×10
−2.333 33	0.5167	0.3662	3.5314	0.3083×10
−4.000	0.9863	0.5781	6.2573	0.9215×10
−9.000	1.9615	0.8854	1.139×10	0.5445×10^2
-10^{-5}	4.2894	1.3093	2.240×10	$\sim 1 \times 10^{10}$

$K_{33}(0)$ and $Q_3(0)$ together with the density expansion coefficient β_2 and α_2 (see (3.2)) for the static conductivity and the diffusion coefficient respectively.

4. Discussions and comparison with computer simulations

In the previous sections we have calculated the coefficients α_l and β_l of the $O(c^l)$ term ($l = 1, 2$) in the density expansion of the diffusion coefficient and the static conductivity respectively. The results for α_1 and β_1 are given through (3.2) and those for α_2 and β_2 are listed in table 2 for several values of b, where $\sigma = 1 - b$ is the hopping rate into an impurity site. Positive (negative) b values correspond to site impurities that are poorer (better) conductors with $\sigma < 1$ ($\sigma > 1$) than the conducting sites of the original host lattice without impurities ($c = 0$).

The low-density coefficient in the c expansion can also be used for high densities because of a symmetry property relating c and $1 - c$. It is based on the mapping (Ernst *et al* 1987) $\{c, \sigma\} \Leftrightarrow \{c' = 1 - c, \sigma' = 1/\sigma\}$ implying $b' = b/(b-1)$ and gives the relation

$$D(c, \sigma) = \sigma D(1 - c, 1/\sigma). \tag{4.1}$$

With the help of this result we have plotted in figure 1 the [1, 4], [3, 2] and [4, 1] Padé approximants to $D(c, \sigma)/D(0, \sigma) = 4D(c, \sigma)$ for values of $\sigma = 1 - b$ in the interval 0.1 (0.1) 1.0. We did not include the [2, 3] Padé approximant, because for $\sigma \leqslant 0.3$ it has poles for $0 < c < 1$. For the percolation case $\sigma = 0$ we have presented the quadratic

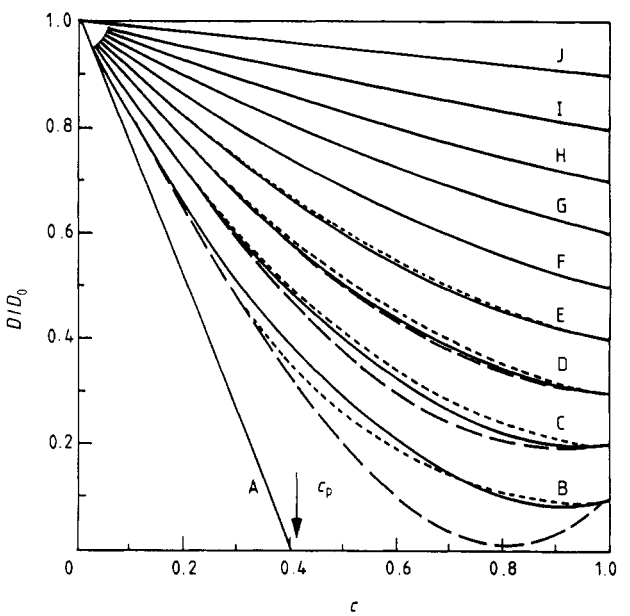

Figure 1. Diffusion coefficient $D(c)/D(0) = 4D(c)$ against impurity concentration c for several values of the impurity conductance $\sigma = 1 - b$ with $0 \leqslant \sigma \leqslant 1$ on a 2D square lattice with site disorder (A, $\sigma = 0$; B, $\sigma = 0.1$; C, $\sigma = 0.2$; D, $\sigma = 0.3$; E, $\sigma = 0.4$; F, $\sigma = 0.5$; G, $\sigma = 0.6$; H, $\sigma = 0.7$; I, $\sigma = 0.8$; J, $\sigma = 0.9$). Broken, full and dotted curves represent [1, 4], [3, 2] and [4, 1] Padé approximants, respectively. For $\sigma = 0$ the low-density expansion, up to $O(c^2)$ included, has been presented. The arrow indicates the percolation threshold.

approximant $4D(c, 0) = 1 + \alpha_1 c + \alpha_2 c^2$. The first observation, when comparing these results with corresponding predictions in the bond disorder problem (Ernst *et al* 1987), is that there is a much stronger density dependence in the present site disorder case. The error bars, estimated by comparing the various Padé approximants, are quite large for $\sigma \leqslant 0.2$. We also note that the $O(c^2)$ coefficient for the diffusion coefficient, $\alpha_2(b)$, is vanishing for $b = 1 - \sigma \simeq 0.850$, and next reaches a relative maximum $\alpha_2 = 0.2059$ at $b \simeq 0.654$ and again vanishes for $b = 0$ (pure case). Similarly, the $O(c^2)$ coefficient for the conductivity, $\beta_2(b)$, shows a relative maximum $\beta_2 = 1.427$ at $b = 0.917$ and vanishes at $b = 0$ too. For $b \to -\infty (\sigma \to +\infty)$ the quantities determining the conductivity approach a finite limit, e.g. $\beta_1 \simeq 2/I(0) = 2\pi/(\pi - 2)$ and so do $K_{33}(0)$, $Q_3(0)$ and β_2, as can be seen from equations (3.10)-(3.12). Since, for $b < 0$, $\Sigma(c) = \langle\psi\rangle D(c) = (1 + |b|c)D(c)$, the density expansion of $D(c)$ is only meaningful for $c \ll |b|^{-1}$. For $\sigma \gg 1$ one does not recover the standard termite problems (Hong *et al* 1986). Here, when moving on a connected cluster of 'superconducting' sites (with $\sigma \gg 1$), the RW makes on the average a jump every $1/\sigma$ time units (fast timescale). After an average number of the order of σ jumps, i.e. on average once per unit of time, the RW leaves the superconducting cluster and jumps to a perimeter site (intermediate timescale). However, the ratio of the probability for jumping back to a superconducting neighbour site over the probability for wandering off into normal conducting region is of the order of σ. Thus only on a timescale of about σ time units (long timescale) can one measure a non-vanishing mean square displacement in the 'normal conducting' region. The standard termite problems have two timescales.

At low impurity concentrations, i.e. to linear order in the impurity concentration, where only isolated 'superconducting' sites occur, the long timescale is absent. However, the long timescale enters in our considerations, because we consider not only $O(c)$ terms but also $O(c^2)$ terms. They come from impurity pairs and contain dimer configurations of two NN impurities as the most important terms.

Furthermore, the site problem under consideration has no simple interpretation in terms of an electric network, since the rate constant across a bond bordered by an impurity site and an impurity free site is $\sigma = 1 - b$ in one direction and unity in the opposite direction. If the bond is bordered by two impurity free (or impurity) sites, the rate constant is 1 (or σ) in both directions.

Computer simulations and theoretical results only seem to exist for the percolation case, where $\sigma = 0$ or $b = 1$. Our results for the conductivity

$$\Sigma(c) = \tfrac{1}{4}(1 - \pi c + 1.2858c^2 + \ldots) \tag{4.2}$$

are in close agreement (Nieuwenhuizen *et al* 1986) with the computer simulations of Harris and Kirkpatrick (1977), and with the intuitive approximation of Watson and Leath (1974) $\Sigma(c) = \frac{1}{4}(1 - \pi c + \pi c^2/2)$ and we refer to the appropriate figure of Nieuwenhuizen *et al* (1986) for a detailed comparison of all the above results. The Watson-Leath contribution is contained in our theory in the term $Q_3(0)$ defined in (1.3), which describes certain contributions from two impurities on nearest-neighbour sites. The Watson-Leath approximation is obtained by neglecting $g(\rho_1, 0)$ in the denominator of $Q_3(0)$ and yields $Q_3^{WL}(0) = t_3(0)a_3(\rho_1) = \pi/8$. Erasing the term $g(\rho_1, 0)$ in (1.3) implies neglecting all repeated crossings of the RW between two nearest-neighbour sites.

There exist more computer simulations on the present model, but they do not allow a meaningful comparison since they are performed at the percolation threshold $c = c_p$ in 2D (Majid *et al* 1984) or 3D (Seifert and Suessenbach 1984) and refer to critical exponents. Computer simulations of high precision have been carried out by Frenkel

(1987) for the diffusion coefficient at impurity concentrations of 1, 2.5, 5, 10 and 15%, where our theoretical results predict

$$D(c) = \tfrac{1}{4}[1 - (\pi - 1)c - 0.8558\, c^2 + \ldots] \tag{4.3}$$

and where Frenkel finds $\alpha_2 = -0.78 \pm 0.04$. In figure 2 we have compared our exact density expansion (4.2) with an approximate result of Keyes and Lyklema (1982), and with the short-time or Enskog value of the diffusion coefficient $D_E = \Phi(\infty, c) = (1 - c)/4$. The last result simply represents the diffusion coefficient on an average (uniform) lattice with a fraction $(1 - c)$ of available sites. The result of Keyes and Lyklema is based on a self-consistent ring-kinetic equation that only takes into account a single return of the RW to an impurity site, and not all possible 'repeated ring collisions'. At low densities this corresponds to a linearisation of (2.4) in $I(0)$, and leads to the incorrect low-density form (curve B):

$$D_R(c) \simeq \tfrac{1}{4}[1 - c(3 - 4/\pi) + \ldots] \tag{4.4}$$

Our result for $D(c)$, exact to $O(c^2)$, vanishes at $c \simeq 0.402$, very close to the percolation threshold $c_p = 1 - p_c = 0.4072 \pm 0.0006$ (Saleur and Derrida 1985) for site percolation on a square lattice. The $O(c)$ approximation in (4.2) would vanish at $c \simeq 0.467$, and the result of Keyes and Lyklema vanishes approximately at $c \simeq 0.6$. It should be mentioned further that the effective medium approximation gives poor results for the site percolation model (Harris and Kirkpatrick 1977), but does very well for the bond percolation model (Kirkpatrick 1973, Ernst *et al* 1987). This may be caused by the strong density dependence of the conductivity and diffusion coefficient in site-disordered models, yielding large values of α_2 and β_2.

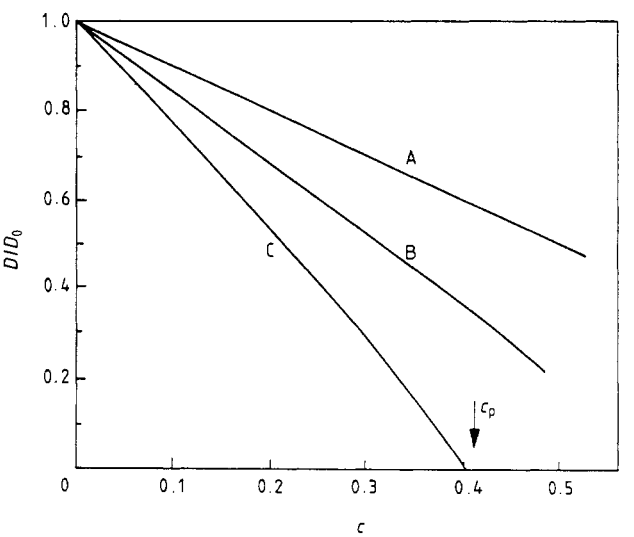

Figure 2. Comparison of different results for the diffusion coefficient $D(c)$ as a function of impurity concentration for the percolation model ($\sigma = 0$ or $b = 1$). Curve A: the Enskog or short time diffusion coefficient $D_E = (1 - c)/4$; curve B: ring approximation $D_R(c)$ in (4.4) of Keyes and Lyklema; curve C: $D(c)$ from our density expansion up to $O(c^2)$. Note that $D(c)$, as given by curve C, vanishes close to the threshold value $c_p = 0.4072 \pm 0.0006$ for site percolation on a 2D square lattice.

In conclusion, we have critically examined the available information on the 2D site percolation and compared it with our exact results. We further conclude that kinetic theory methods provide practical means for calculating transport coefficients in disordered systems at low impurity concentrations, where no other methods of practical use seem to be available. Our numerical method for evaluating lattice sums converges rapidly. Summing the contributions from the 24 sites closest to the origin ($|n_x|+|n_y| \leq 4$) enables us to obtain the transport coefficient with a relative accuracy of $1:10^{-4}$. In fact, NNN sites with $|n_x|+|n_y| \leq 2$ determine the lattice sum with a 5% accuracy, as illustrated in table 1.

Acknowledgments

It is a pleasure to thank D Frenkel for many stimulating discussions. One of us (MHE) wants to thank IPST of the University of Maryland for its hospitality and financial support during the summer and autumn of 1986 where part of this work was carried out. One of us (ThMN) acknowledges support in part from the 'Stichting voor Fundamental Onderzoek der Materie' (FOM), which is sponsored by the 'Stichting voor Zuiver-Wetenschappelijk Onderzoek' (ZWO).

Appendix 1

A1.1. Properties of lattice Green functions

The lattice Green functions $g(n, z)$, defined in (1.4), are 5×5 matrices labelled with i, $j \in \{0, 1, 2, 3, 4\}$. However, their zeroth row vanishes identically on account of (1.4a) and their zeroth column never enters in our calculation. We can restrict ourselves to 4×4 matrices with labels $i, j \in \{1, 2, 3, 4\}$:

$$g_{ij}(n, z) = \begin{cases} \int gc(n)\tilde{e}_i e_j & i, j \in \{1, 2\} \\ -\int gc(n) e_i e_j & i, j \in \{3, 4\} \\ \int gs(n)\tilde{e}_i e_j & i \in \{1, 2\}, j \in \{3, 4\} \\ \int gs(n) e_i e_j & i \in \{3, 4\}, j \in \{1, 2\}. \end{cases} \tag{A1.1}$$

The components of the 4-vectors $\tilde{\boldsymbol{e}} = \{e_1 - 1, e_2, e_3, e_4\}$ and $\boldsymbol{e} = \{e_1, e_2, e_3, e_4\}$ are defined in (1.4). The integration symbol is an average over the first Brillouin zone q_x, $q_y \in [-\pi, \pi]$ with weight $(4\pi^2)^{-1}$. Furthermore

$$g = [z + \omega(q)]^{-1} = [z + e_1(q)]^{-1}$$

$$c(n) = \cos(n_x q_x + n_y q_y)$$

$$s(n) = \sin(n_x q_x + n_y q_y).$$

On account of the square symmetry the matrix elements in (A1.1) obey the symmetry properties discussed in appendix 2 of I. They allow us to restrict ourselves to sites $n = \{n_x, n_y\}$ with $n_x \geq n_y \geq 0$.

We start by calculating averages over products of basis vectors, which can be expressed in terms of a few independent integrals:

$$f_0(z)=\int g \qquad f_1(z)=\int ge_3^2 \qquad f_9(z)=\int ge_3^2e_4^2\ldots. \tag{A1.2}$$

The first two are in fact sufficient to calculate all matrix elements of n at the origin and at its NN sites; with the additional integral $f_9(z)$ all NNN matrix elements can be calculated, etc. The required integrals are

$$\begin{aligned}
f_2(z)&=\int ge_1=1-zf_0(z)\\
f_3(z)&=\int ge_1^2=1-zf_2(z)\\
f_4(z)&=\int ge_2^2=2f_2(z)-f_3(z)-f_1(z)\\
f_5(z)&=\int ge_1^3=\tfrac{5}{4}-zf_3(z)\\
f_6(z)&=\int ge_1e_2^2=\tfrac{1}{4}-zf_4(z)\\
f_7(z)&=\int ge_1e_3^2=\tfrac{1}{2}-zf_1(z)\\
f_8(z)&=\int ge_2e_4^2=2f_4(z)-2f_6(z).
\end{aligned} \tag{A1.3}$$

In deriving these equations we have used the identities

$$g^{-1}=z+e_1 \qquad 2e_2^2+e_3^2+e_4^2=4e_1-2e_1^2$$
$$e_2(e_4^2-e_3^2)=4e_2^2(1-e_1).$$

In the applications of this paper only $g(n,0)\equiv g(n)$ is needed. In the limit $z\to 0$ all $f_l(0)$ are finite except $f_0(z)$ which is of $O(\ln z)$. For the independent integrals in (A1.2) we quote the values

$$f_1(0)=[e_3^2]=2-4/\pi \qquad f_9(0)=[e_3^2e_4^2]=2-16/(3\pi). \tag{A1.4}$$

The first integral was calculated in (2.2) and (2.3); the second can be obtained in a similar manner. In (A1.4) we introduced an average $[\ ]$ over the 1BZ; we further need a second one $\langle\ \rangle$. Their definitions are

$$[u]=\int (e_1(q))^{-1}u(q) \qquad \langle u\rangle=\int u(q)$$

and obey the relation $[ue_1]=\langle u\rangle$. With the help of these relations, together with (1.4*b*) and (A1.1), we derive a recursion relation of the same structure as derived by Morita and Horiguchi (1971):

$$\langle e^{-iqn}\tilde{e}e\rangle=g(n_x,n_y)-\tfrac{1}{4}[g(n_x+1,n_y)+g(n_x-1,n_y)+g(n_x,n_y+1)+g(n_x,n_y-1)]. \tag{A1.5}$$

The matrix on the LHS of (A1.5) is only non-vanishing for $n=\{0,0\}$, $\{1,0\}$, $\{1,1\}$ and $\{2,0\}$ (recall the previous restriction $n_x \geqslant n_y \geqslant 0$), and can be trivially calculated.

A relation between the elements of $\boldsymbol{g}(n)$ can be deduced from the second identity below (A1.4). The result is

$$2g_{22}(n) = 2\delta_{n0} + \tfrac{1}{2}\delta_{n\rho_1} + g_{33}(n) + g_{44}(n) \tag{A1.6}$$

where $\rho_1 = \{1,0\}$ is a NN-lattice vector.

Next we calculate the first column of $\boldsymbol{g}(n, z)$ at $z=0$:

$$g_{j1}(n) = \langle e^{-iqn}\, \tilde{e}_j \rangle = \begin{cases} a_j(\rho) & n=\rho \\ 0 & n \neq \rho \end{cases} \tag{A1.7}$$

where $\boldsymbol{a}(\rho_1)$ is a 4-vector with components

$$\boldsymbol{a}(\rho_1) = \tfrac{1}{4}(-1, 1, 2, 0). \tag{A1.8}$$

The 4-vectors $\boldsymbol{a}(\rho_i)$ with $i=2, 3, 4$ can be deduced from square symmetry, as discussed in appendix 2 of I. An important consequence of (A1.1) for $n \neq \rho$ and $n \neq 0$ (see § 3.2) is that only elements of $\boldsymbol{g}(n)$ in the (234) subspace are needed. Therefore only those elements will be calculated.

A1.2. Static values g(n)

We denote the static values at $z=0$ as $\boldsymbol{g}(n;0) \equiv \boldsymbol{g}(n)$. For the site $n=\{0,0\}$ the matrix is diagonal in the (1234) subspace and we derive from (A1.2)-(A1.4)

$$g_{jj}(\{0,0\}) = \begin{cases} [(e_1-1)e_1] = 0 & (j=1) \\ [e_2^2] = -1 + 4/\pi & (j=2) \\ -[e_3^2] = -2 + 4/\pi & (j=3,4). \end{cases} \tag{A1.9}$$

These values also suffice to calculate the $\boldsymbol{t}$ matrix elements, introduced in (1.5*a*, *b*):

$$\begin{aligned} t_1(0) &= b \\ t_2(0) &= (1/b + 1 - 4/\pi)^{-1} \\ t_3(0) &= t_4(0) = (2/b - 2 + 4\pi)^{-1}. \end{aligned} \tag{A1.10}$$

For the NN site $n=\rho_1=\{1,0\}$ we find similarly from (A1.2)-(A1.4)

$$\boldsymbol{g}(\{1,0\}) = \begin{bmatrix} -\frac{1}{4} & \frac{5}{4} - 4/\pi & -\frac{3}{2} + 4/\pi & 0 \\ \frac{1}{4} & -\frac{5}{4} + 4/\pi & \frac{5}{2} - 8/\pi & 0 \\ \frac{1}{2} & \frac{5}{2} - 8\pi & 12/\pi - 4 & 0 \\ 0 & 0 & 0 & 1 - 4/\pi \end{bmatrix}. \tag{A1.11}$$

In table 3 we have listed the elements $g_{ij}(n) = g_{ji}(n)$ in the (234) subspace for sites $N=\{n_x, n_y\}$ with $|n_x| + |n_y| \leqslant 4$. So far we have analytic expressions for $\boldsymbol{g}(\{n_x, n_y\})$ in the (234) subspaces for the 40 sites nearest to the origin. Since the lattice sums converge very rapidly (see § 3.3), these terms yield a fairly good estimate. If more accurate results are needed (see I), then one needs to calculate $\boldsymbol{g}(\{n_x, n_y\})$ for more distant sites, and the analytic methods become too cumbersome. Therefore we have calculated the relevant matrix elements numerically. To illustrate the method we consider $g_{33}(n)$ for $n \neq 0$ and $n \neq \rho$, and obtain from (A1.1):

$$g_{33}(\{n,m\}) = -(2\pi)^{-2} \int_{-\pi}^{\pi} \mathrm{d}x_1 \int_{-\pi}^{\pi} \mathrm{d}x_2\, s_1 \cos(nx_1) \cos(mx_2)/(1 - c_1/2 - c_2/2) \tag{A1.12}$$

Table 3. Matrix elements $g(\{n_x, n_y\})$.

n_x \ n_y	0	1	2	3	4
$g_{22}(\{n_x, n_y\}) = g_{22}(\{n_y, n_x\})$					
0	$-1+4/\pi$	$-\frac{5}{4}+4/\pi$	$-8+76/3\pi$	$-42+132/\pi$	$-224+10\,556/15\pi$
1	$-\frac{5}{4}+4/\pi$	$2-20/3\pi$	$\frac{11}{2}-52/3\pi$	$32-1508/15\pi$	
2	$-8+76/3\pi$	$\frac{11}{2}-52/3\pi$	$-4+188/15\pi$		
3	$-42+132/\pi$	$32-1508/15\pi$			
4	$-224+10\,556/15\pi$				
$g_{33}(\{n_x, n_y\}) = g_{44}(\{n_y, n_x\})$					
0	$-2+4/\pi$	$1-4/\pi$	$+2-20/3\pi$	$8-76/3\pi$	$34-1604/15\pi$
1	$-4+12/\pi$	$2-20/3\pi$	$-\frac{1}{2}+4/3\pi$	$-2+92/15\pi$	
2	$-18+172/3\pi$	$\frac{23}{2}-36/\pi$	$-4+188/15\pi$		
3	$-92+868/3\pi$	$66-1036/5\pi$			
4	$-482+7572/5\pi$				
$g_{23}(\{n_x, n_y\}) = -g_{24}(\{n_y, n_x\})$					
0	0	0	0	0	0
1	$-\frac{5}{2}+8/\pi$	$1-8/3\pi$	$-\frac{5}{2}+8/\pi$	$-10+472/15\pi$	
2	$-12+112/3\pi$	$\frac{17}{2}-80/3\pi$	$-1+16/5\pi$		
3	$-62+584/3\pi$	$46-2168/15\pi$			
4	$-328+5152/5\pi$				
$g_{34}(\{n_x, n_y\}) = g_{43}(\{n_y, n_x\})$					
0	0	0	0	0	0
1	0	$2-16/3\pi$	$\frac{7}{2}-32/3\pi$	$16-752/15\pi$	
2	0	$\frac{7}{2}-32/3\pi$	$-4+64/5\pi$		
3	0	$16-752/15\pi$			
4	0				

where $s_1 = \sin x_1$, $c_1 = \cos x_1$ and $c_2 = \cos x_2$. After the substitution $w = \exp(ix_1)$ the contour integral over the unit circle in the complex w plane can be performed and yields for $n \neq 0$ and $n \neq \rho$:

$$g_{33}(\{n, m\}) = (2/\pi)\int_0^\pi dx_1 \cos(mx_1)[\ ]^n[(1-c_1)(3-c_1)]^{1/2} \qquad \text{(A1.13)}$$

with

$$[\ ] = 2 - c_1 - [(1-c_1)(3-c_1)]^{1/2}.$$

Similar expressions can be derived for all relevant matrix elements in the (234) subspace. However, it follows from the recursion relation (A1.5) that, once $g(\{n_x, n_y\})$ is known for $n_x \leq M$ and $n_y = 0$, then $g(n)$ can be calculated for all sites with $|n_x| + |n_y| \leq M$. For sites $n = \{n_x, 0\}$ with $n_x \geq 2$ the matrix $g(n)$ has the general form (see (A1.6)):

$$g(\{n, 0\}) = \begin{bmatrix} (a+b)/2 & c & 0 \\ c & a & 0 \\ 0 & 0 & b \end{bmatrix}. \qquad \text{(A1.14)}$$

In the expression (A1.1) for these matrix elements one can carry out one integration analytically, as in (A1.12). One finds the following results, which have been used for

performing the numerical integrations:

$$g_{33}(\{n,0\}) = (2/\pi)\int_0^\pi \mathrm{d}x_1[\ ]^n[(1-c_1)(3-c_1)]^{1/2}$$
$$g_{44}(\{n,0\}) = -(2/\pi)\int_0^\pi \mathrm{d}x_1[\ ]^n s_1^2[(1-c_1)(3-c_1)]^{-1/2} \qquad \text{(A1.15)}$$
$$g_{23}(\{n,0\}) = -(2/\pi)\int_0^\pi \mathrm{d}x_1[\ ]^n(1-c_1).$$

The expression [ ], defined in (A1.13), is always positive and smaller than unity. Hence the formulae (A1.15) are suitable for numerical integration. We also point out that the alternative expression, obtained from (A1.12) by setting $n_x = 0$, namely

$$g_{33}(\{0,m\}) = g_{44}(\{m;0\}) = (2/\pi)\int_0^\pi \mathrm{d}x_1 \cos(mx_1)[(1-c_1)(3-c_1)]^{1/2}$$

is not suitable for numerical integration, because its integrand rapidly oscillates with increasing m.

A1.3. Behaviour at large distances

The asymptotic large-n behaviour of the matrix $\boldsymbol{g}(\{n_x, n_y\})$ in the (234) subspace can be obtained most conveniently from expressions of the form (A1.12) by changing to a new 'integration variable χ', defined through $\cosh\chi = 2 - \cos x_1$. The factor $[\ ]^n$ transforms into $\exp(-n_x\chi)$. The dominant behaviour for $n_x \geq n_y \geq 0$ and $n_x \gg 1$ is obtained by expanding the remaining part of the integrand around $\chi = 0$, and is for a site $\{n, m\}$:

$$g_{22}(\{n,m\}) = g_{22}(\{m,n\}) \simeq (3/\pi)(n^4 - 6n^2m^2 + n^4)/(n^2+m^2)^4$$
$$g_{23}(\{n,m\}) = g_{24}(\{m,n\}) \simeq -(2/\pi)n(n^2-3m^2)/(n^2+m^2)^3$$
$$g_{33}(\{n,m\}) = g_{44}(\{m,n\}) \simeq (2/\pi)(n^2-m^2)/(n^2+m^2)^2 \qquad \text{(A1.16)}$$
$$g_{34}(\{n,m\}) = g_{43}(\{m,n\}) \simeq (4/\pi)nm/(n^2+m^2)^2.$$

These matrix elements decrease respectively as d^{-4}, d^{-3}, d^{-2}, d^{-2} for large d, where $d^2 = n^2 + m^2$.

Appendix 2

We evaluate lattice sums $\Sigma_n\,(\boldsymbol{g}(n;z)\boldsymbol{\lambda}\boldsymbol{g}(n;z))_{33}$, where $\boldsymbol{g}$ and $\boldsymbol{\lambda}$ are 4×4 matrices with labels $i, j \in \{1,2,3,4\}$ and where $\boldsymbol{\lambda}$ is a diagonal matrix with elements $\lambda_{ij} = \lambda_i\delta_{ij}$. We obtain from (1.4), using the definition $g(q) = (z+\omega(q))^{-1}$

$$\sum_n (\boldsymbol{g}(n,z)\boldsymbol{\lambda}\boldsymbol{g}(n,z))_{33}$$
$$= \sum_{j=1}^4 \sum_n \int_q \int_{q'} \exp[-\mathrm{i}(q-q')n]g(q)g(q')e_3(q)e_j(q)\lambda_j\tilde{e}_j(q')e_3(q')$$
$$= \sum_{j=1}^4 \lambda_j\theta_j(z) \qquad \text{(A2.1)}$$

where

$$\theta_1(z) = \int g^2 e_3^2 e_1(e_1 - 1)$$
$$\theta_j(z) = \int g^2 e_3^2 e_j^2 \qquad (j = 2, 3, 4). \tag{A2.2}$$

In (A2.1) we also used the relation $\Sigma_n \exp(iqn) = N\delta_{q0}$. The coefficients can be expressed in the integrals $f_l(z)$ of (A1.2) and (A1.3) in appendix 1 via a partial integration using $dg(q)/dq_x = -\frac{1}{2}e_3(q)g^2(q)$. The result is

$$\begin{aligned}
\theta_1(z) &= \{1 + z(d/dz)\}(f_7(z) - f_1(z)) \\
\theta_2(z) &= 6(f_4(z) - f_6(z)) \\
\theta_3(z) &= 6(f_1(z) - f_7(z) - f_8(z)) \\
\theta_4(z) &= 2(f_1(z) - f_7(z) + f_8(z)).
\end{aligned} \tag{A2.3}$$

The values at $z = 0$ are obtained from (A1.2)-(A1.4):

$$\begin{aligned}
\theta_1(0) &= 4/\pi - \tfrac{3}{2} & \theta_2(0) &= 24/\pi - \tfrac{15}{2} \\
\theta_3(0) &= 24 - 72/\pi & \theta_4(0) &= -2 + 8/\pi.
\end{aligned} \tag{A2.4}$$

In the body of the paper we apply (A2.1) for the calculation of $\Sigma\, \boldsymbol{r}^2(n) = \Sigma\, \boldsymbol{g}(n)\boldsymbol{t}\boldsymbol{g}(n)\boldsymbol{t}$, where $\boldsymbol{t}$ is diagonal. In the lattice sums to be considered the term $\boldsymbol{r}(0) = \boldsymbol{g}(0)\boldsymbol{t}$, involving site $n = 0$, is missing and has to be subtracted from the final sums. Since the matrix $\boldsymbol{g}(0)$, calculated in (A1.9), is diagonal we only need its (33) element, given by $g_{33}(0) = 4/\pi - 2$. In this way we obtain

$$\begin{aligned}
\sum_{n \neq 0} (\boldsymbol{t}\boldsymbol{r}^2(n))_{33} &= t_3^2 \sum_{j=1}^{4} t_i \theta_j - t_3^2 (g_{33}(0))^2 \\
&= t_3^3(18 - 48/\pi - 16/\pi^2) + t_3^2 t_2(24/\pi - \tfrac{15}{2}) + t_3^2 t_1(4/\pi - \tfrac{3}{2}).
\end{aligned} \tag{A2.5}$$

References

Ernst M H, van Velthoven P F J and Nieuwenhuizen Th M 1987 *J. Phys. A: Math. Gen.* **20** 949
Frenkel D 1987 *Phys. Lett.* **121** 385
Harris A B and Kirkpatrick S 1977 *Phys. Rev.* B **16** 542
Haus J W and Kehr K W 1987 *Phys. Rep.* **150** 262
Hong D C, Stanley H E, Coniglio A and Bunde A 1986 *Phys. Rev.* B **33** 4564
Izyumov Y 1966 *Proc. Phys. Soc.* **87** 505
Keyes T and Lyklema J W 1982 *J. Stat. Phys.* **27** 487
Kirkpatrick S 1973 *Rev. Mod. Phys.* **45** 574
Lifshitz I M 1964 *Adv. Phys.* **13** 483
Majid I, Ben-Avraham D, Havlin S and Stanley H E 1984 *Phys. Rev.* B **30** 1626
Morita T and Horiguchi T 1971 *J. Math. Phys.* **12** 981
Nieuwenhuizen Th M, van Velthoven P F J and Ernst M H 1986 *Phys. Rev. Lett.* **57** 2477
—— 1987 *J. Phys. A: Math. Gen.* **20** 4001
Saleur H and Derrida B 1985 *J. Physique* **46** 1043
Seifert E and Suessenbach M 1984 *J. Phys. A: Math. Gen.* **17** L703
Watson B P and Leath P J 1974 *Phys. Rev.* B **9** 4893